


## FOLIAR APPLICATION OF SUGARCANE MOLASSES CAN ALLEVIATE STRESSFUL CONDITION IN GLYCINE MAX (L.) MERR. CROP UNDER FIELD CONDITIONS

 <https://doi.org/10.56238/arev7n1-038>

Date of submission: 03/12/2024

Date of publication: 03/01/2025

**Agna dos Santos Moreira<sup>1</sup>, Mateus Dias Duarte<sup>2</sup>, Joyce de Sousa Cordeiro<sup>3</sup>, Ana Larissa Pereira da Silva<sup>4</sup>, Nahor Daniel Ribeiro Diniz<sup>5</sup>, Wallace de Paula Bernado<sup>6</sup>, Tiago Cunha Rocha<sup>7</sup>, Járison Cavalcante Nunes<sup>8</sup>, Tiago Massi Ferraz<sup>9</sup>, Fabrício de Oliveira Reis<sup>10</sup>, Fábio Afonso Mazzei Moura de Assis Figueiredo<sup>11</sup>, Eliemar Campostrini<sup>12</sup>, José Cochicho Ramalho<sup>13</sup> and Weverton Pereira Rodrigues<sup>14</sup>**

### ABSTRACT

The objective of the present study was to investigate the effects of sugarcane molasses application at 2 days (D2) and 7 days (D7) after precipitation after a period of drought stress on some physiological, growth, and yield parameters of soybean under field conditions. The experiment was set to obtain 14 plants per meter of row, and considered two treatments: molasses application at 2 days (D2) and 7 days (D7) after precipitation, after ca. 1 month without rainfall. Twenty days after the second application, thermographic and chlorophyll a fluorescence measurements were taken at the reproductive stage (R5 - early seed filling). Measurements were conducted between 12:00 and 14:00, representing the hottest hours of the day, on fully expanded leaves. Additionally, plant growth and yield measurements were

---

<sup>1</sup> Undergraduate student  
State University of the Tocantina Region of Maranhão

<sup>2</sup> Undergraduate student  
State University of the Tocantina Region of Maranhão

<sup>3</sup> Undergraduate student  
State University of the Tocantina Region of Maranhão

<sup>4</sup> Graduated  
State University of Maranhão

<sup>5</sup> Graduated  
State University of Maranhão

<sup>6</sup> Master  
North Fluminense State University

<sup>7</sup> PhD  
State University of the Tocantina Region of Maranhão

<sup>8</sup> PhD  
State University of the Tocantina Region of Maranhão

<sup>9</sup> PhD  
State University of Maranhão

<sup>10</sup> PhD  
State University of Maranhão

<sup>11</sup> PhD  
State University of Maranhão

<sup>12</sup> PhD  
North Fluminense State University

<sup>13</sup> PhD  
University of Lisbon and NOVA University Lisbon

<sup>14</sup> PhD  
State University of the Tocantina Region of Maranhão

taken from the same plants at the reproductive stage R7. The plot treated with sugarcane molasses application at D2 showed increased productivity (ca. 58%) due to higher stomatal conductance as reflected by water stress and relative stomatal conductance thermal index conditions.

**Keywords:** Abiotic Stress. Alleviation. Byproduct. Sustainability.

## INTRODUCTION

With the global population approaching 10,000 million by 2050, food and energy demand is expected to greatly increase (Fróna *et al.* 2019; Pais *et al.* 2020) with the need to greatly increase global food production by about 60-70% (Powell *et al.*, 2012; FAO, 2016). It is estimated that wheat, rice, maize, and soybean provide about 2/3 of global human caloric intake (Zhao *et al.* 2017), with soybean contributing mainly by being incorporated into animal feeds (with a high protein value) and through refined soybean oil (Fischer *et al.* 2014).

In addition to population growth, climate changes (CC) amplify the contemporary challenges of ensuring food security. In fact, projections indicate that concentrations could exceed 1,000  $\mu\text{L CO}_2 \text{ L}^{-1}$  by 2100, potentially raising global temperatures up to 5.7 °C in a worst estimate (IPCC, 2023). This increase is also expected to intensify the frequency of extreme weather events, including heat waves, prolonged droughts, and heavy rainfalls (IPCC 2023). Such CC, particularly rising temperatures and droughts, are anticipated to reduce crop yields globally (Gupta *et al.* 2020).

The global soybean production for the 2022/2023 marketing year was approx. 378.6 million metric tons (USDA 2024), whereas in 2023/2024 season, Brazil produced approx. 147 million metric tons, with an average of 3,202 kg yielded per hectare over 46 million hectares (CONAB 2024). However, soybean is considered quite vulnerable to increasingly CC stressful conditions, especially drought (Arya *et al.* 2021), and heat, with global yields reduction of 3.1% (on average) per each °C increase, although with a stronger impact of 6.8% in the United States (Zhao *et al.*, 2017). Under such CC context we are facing a complex challenge regarding the need of increasing food production to follow the rising food demand of a growing population, under worsening climate conditions that could threaten food security unless effective strategies are adopted (Diffenbaugh and Burke 2019; Pais *et al.* 2020).

A recent study has suggested that endogenous food-borne carbon dots derived from sugar beet molasses may help mitigate the negative impacts of drought stress (Kara *et al.* 2023). Therefore, this type of management practices, may offer additional resilience against abiotic stress, although such a strategy has not yet been studied in soybean cultivation, namely by the use of sugarcane molasses, which is rich in various nutrients and organic compounds, in addition to being inexpensive as it is a byproduct of sugar production. Such strategies require a comprehensive understanding of plant physiological responses, in

order to determine the optimal timing for application, depending on the duration and intensity of the drought stress.

Several techniques are employed to measure direct physiological traits, such as photosynthesis and stomatal conductance, but these are often time-intensive, limiting their use for studying a substantial number of genotypes under field conditions. Additionally, the relatively high cost of these instruments restricts accessibility (Zia *et al.* 2013). Consequently, the use of tools that can indirectly reflect physiological changes has grown markedly, given their affordability and rapid data collection, which facilitates their application to a larger number of genotypes in field conditions (Galiene *et al.* 2021). Utilizing various measurements of chlorophyll *a* fluorescence emission enables rapid and non-invasive detection of potential damage to the photochemical machinery caused by abiotic stress factors (Kalaji *et al.* 2016). In addition to chlorophyll *a* fluorescence, thermal imaging analysis is widely recognized to evaluate plant stress status, owing to the strong correlation between leaf temperature and the fluxes of CO<sub>2</sub> and water vapor, both regulated by stomatal conductance (Sirault *et al.* 2009; Gutierrez *et al.* 2018). Therefore, this tool is currently used for accurate estimations of biomass and productivity (García-Tejero *et al.* 2017). Furthermore, thermal imaging allows for canopy-scale evaluation/integration, with advantages over single leaf-scale measurements (García-Tejero *et al.* 2017). In terms of abiotic stresses, an increase in the frequency of vapor pressure deficit (VPD) events is anticipated due to atmospheric warming and reduced relative humidity. This scenario of 'atmospheric drought' may, depending on the plant's hydraulic capacity, result in water stress even when soil moisture is still within a sufficient range (Gilbert *et al.* 2011; Sinclair 2017; Kunert and Vorster 2020).

This study hypothesized that applying a foliar spray of sugarcane molasses shortly after a period (*ca.* 1 month) of absence of rain could aid soybean plants to recover to the potential water deficit while, maintaining a satisfactory yield. Therefore, the research aimed to examine the effectiveness of sugarcane molasses as a potential tool for alleviating abiotic stress in soybean cultivation under commercial field conditions.

## **MATERIAL AND METHODS**

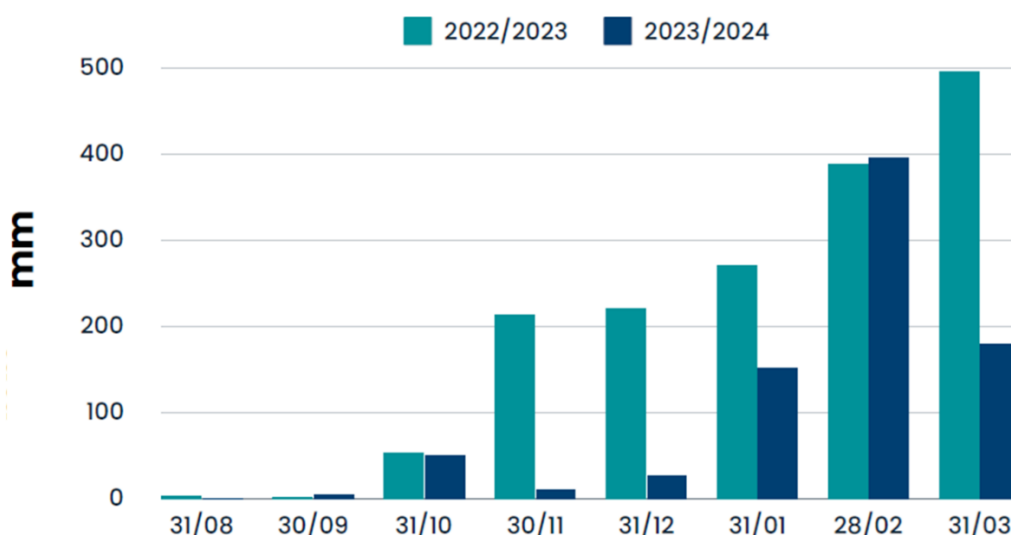
### **PLANT MATERIAL AND EXPERIMENTAL DESIGN**

The experiment was performed *Glycine max* (L.) Merr. cv. Brasmax Olimpo IPRO plants, in Itinga, Maranhão, Brazil (longitude 47°06'48"W and latitude -6°16'23"S). The

local climate is 'Aw' type by the Köppen's classification, with average annual temperature ca. of 27.1°C, annual rainfall of 1,672 mm, and 204.65 m.a.s.l (Alvares *et al.* 2013). Sowing was carried out on December 26, 2023, in a Dystrophic Yellow Latosol. Soil preparation and crop management were implemented following recommended practices in relevant literature, while fertilization was guided by soil analysis to meet the crop's nutrient needs. Seed density was calculated based on germination rates to achieve a target of 14 plants per meter of row, with these rows spaced 0.50 m apart.

A randomized block design was used for the experiment, with two treatments involving sugarcane molasses foliar applications at either 2 days (D2) or 7 days (D7) post-precipitation, with four replication. Each block consisted of eight rows of 9 m long, with data collection focused on the four central rows of three plants each, thus using a total of 48 plants per treatment. Foliar sprays of molasses (1 L ha<sup>-1</sup>) were applied following a 28-day period without rainfall (Figure 1). The first application was carried out on February 5 (42 days after sowing - DAS), and the second application on February 10 (47 DAS), both at the V6 vegetative stage, using a self-propelled sprayer. Twenty days after the second application (66 DAS), the physiological measurements described below were performed at the R5.4 reproductive stage. The growth and yield measurements were taken during the R7 reproductive stage (108 DAS), representing the physiological maturity of the bean at the end of the crop life cycle.

Figure 1 - Precipitation at the experimental site in Itinga, Maranhão, during the 2022/2023 and 2023/2024 growing seasons. Although January in the 2023/2024 growing season received approximately 145.6 mm of rainfall, this volume occurred within the first five days of the month. From January 6<sup>th</sup> to February 2<sup>nd</sup>, no rainfall was recorded. On February 3<sup>rd</sup>, 76.1 mm of rainfall was observed, followed by 38 mm on February 4<sup>th</sup>, with the first application conducted on February 5<sup>th</sup>.



## THERMAL IMAGENS ANALYSIS

At the R5.4 reproductive stage, thermal images were captured using a Flir E8-XT infrared camera (Flir Systems, USA) with the camera emissivity set at 0.96. This focal plane array detector produced images with a resolution of 320 x 240 pixels (76,800 pixels) and an accuracy of  $\pm 2\%$ . For each measurement, the camera was positioned approximately 0.50 m above the plants. The images were stored in the device's memory, and FLIR Tools software version 5.12.17023.2001, Copyright© 2015 FLIR, was used for image processing. Leaf temperature (LT) was measured to obtain the Crop Water Stress Index (CWSI) according to Jones (1999):

$$CWSI = \frac{T_{canopy} - T_{wet}}{T_{dry} - T_{wet}} \quad (\text{Equation 1})$$

An alternative index based on a rearrangement of the energy balance equation, the thermal relative stomatal conductance index ( $I_G$ ), was also used following Jones (1999):

$$I_G = \frac{T_{dry} - T_{canopy}}{T_{canopy} - T_{wet}} \quad (\text{Equation 2})$$

where  $T_{canopy}$  is the representative temperature of the plant's leaves,  $T_{dry}$  is the temperature of a leaf with the abaxial surface coated with petroleum jelly (representing maximum stress, with stomata closed), and  $T_{wet}$  is the temperature of a leaf with the adaxial surface sprayed with water (representing maximum transpiration, with fully open stomata). For index estimation, one plant per replication was selected, where one leaflet received petroleum jelly to mimic maximum stress conditions while another leaflet on the same leaf was sprayed with water to represent maximum transpiration Rodrigues *et al.* (2024).

## CHLOROPHYLL A FLUORESCENCE MEASUREMENTS AND SPAD READINGS

At the R5.4 reproductive stage, chlorophyll *a* fluorescence variables were measured using a non-modulated light fluorimeter, model Pocket Pea (Plant Efficiency Analyzer, Hansatech, King's Lynn, UK). Before each measurement, leaves were dark-adapted for 30 minutes using leaf clips to ensure reaction centers were open (with quinone A (QA) in the oxidized state). After this dark adaptation period, fluorescence was induced by a red light pulse (650 nm) at an intensity of  $3500 \mu\text{mol m}^{-2} \text{s}^{-1}$ , provided by LEDs located in the device

probe. Among the evaluated parameters,  $F_0$  reflects the chlorophyll a emission within the antenna complex of PSII at 50 ms, representing the minimum fluorescence level in dark-adapted leaves (initial fluorescence).  $F_m$  corresponds to the maximum fluorescence achieved under continuous light intensity, representing the peak fluorescence in dark-adapted leaves.  $F_v$ , calculated as the difference between  $F_m$  and  $F_0$ , indicates the maximum potential for photochemical quenching, which occurs within 200–300 ms following the transition from dark to light exposure in photosynthetic material. From the previous parameters, basal quantum yield of non-photochemical processes ( $F_0/F_m$ ), maximum quantum yield of photosystem II ( $F_v/F_m$ ), maximum efficiency of the photochemical process in photosystem II ( $F_0/F_v$ ) were estimated (Strasser *et al.* 2004).

The Performance Index (PI), a highly sensitive metric for assessing the effects of stress-induced changes in PSII activity (Kalaji *et al.* 2016), was determined using the formula:  $PI = (1 - (F_0/F_m)) / M_0 \times (F_m - F_0) / F_0 \times (1 - V_j) / V_j$ . In this context,  $V_j$  represents the relative variable fluorescence at 2 ms, calculated as  $V_j = (F_j - F_0) / (F_m - F_0)$ , where  $F_j$  is the fluorescence intensity at the J step (2 ms).  $M_0$ , the initial slope of fluorescence kinetics, was derived using the equation  $M_0 = 4 \times (F_{300\text{ ms}} - F_0) / (F_m - F_0)$ .

Also at the R5 reproductive stage, SPAD reading was performed on the tagged leaves previously used for chlorophyll a fluorescence measurements, and the same time, using a SPAD-502 Chlorophyll Meter (Minolta Co. Ltd., Osaka, Japan). The average of twelve SPAD readings (four points on each leaflets) was recorded for each leaf.

## GROWTH AND YIELD COMPONENTS TRAITS

At the R7 reproductive stage (108 DAS), plant height was recorded using a graduated ruler, and leaf area (LA) was calculated based on the width and length of the primary leaflet, following the methodology of Richter *et al.* (2014). The leaf area index (LAI) of soybean plants was determined using the following equation (Montgomery, 1911):

$$LAI = \frac{\text{Leaf area per plant} \times \text{plant number per plot}}{\text{Plot area}} \quad (\text{Equation 3})$$

In the field, the number of nodes per plant (NNP) and the number of pods per plant (NPP), the number of beans per plant (NB), and number of beans per pod (NBP) were obtained. After manual harvesting, the beans were oven-dried at 70 °C until they reached a

stable moisture content of 13% (ca. 72 h). Bean mass per plant (BMP), and bean yield (Kg ha<sup>-1</sup>) were obtained.

## STATISTICAL ANALYSIS

With four plots and twelve plants per plot, the experiment was structured as a randomized block design. Data were analyzed using a one-way ANOVA at a 5% significance level. Phenotypic correlations among the variables were also estimated. All statistical analyses were performed using R software (R Core Team, 2021, <https://www.r-project.org/>), employing 'corrplot', and 'Hmisc' packages.

## RESULTS

Results revealed no significant differences in LAI between D2 and D7 treatments, although there was a tendency toward higher values for the D2 (Figure 2). However, NNP, NPP, NB and NBP showed significant differences, with the use of sugarcane molasses in D2 resulting in the highest values compared to D7 treatment. The greater values of yield components in D2 plants resulted in substantial greater productivity for this treatment (ca. 58%) (Table 1).

Figure 2 - Leaf area index, LAI of *G. max* cv. Brasmax Olimpo IPRO plants sprayed with sugarcane molasses at 2 (D2) and 7 (D7) days after the onset of precipitation following a 28-day period without rain, 66 days after sowing (DAS) For each variable, the mean values  $\pm$  SE (n = 4 plants) followed by NS indicates no statistical differences between treatments at a 5% confidence level.

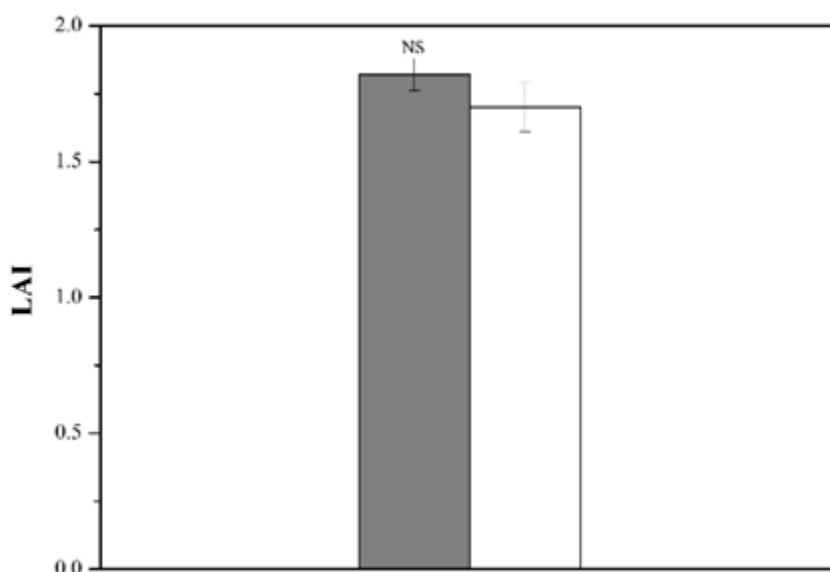




Table 1. Number of nodes per plant (NNP), number of pods per plant (NPP), number of beans per plant (NB), number of beans per pod (NBP), and bean yield of *G. max* cv. Brasmax Olimpo IPRO sprayed with sugarcane molasses at 2 (D2) and 7 (D7) days after the onset of precipitation following a 28-day period without rain. Measurements were taken at 108 DAS.

Variables	D2	D7
NNP	14.50 ± 0.16*	11.96 ± 0.91
NPP	45.14 ± 2.72 *	34.25 ± 0.73
NB	111.94 ± 5.22*	77.31 ± 1.31
NBP	2.49 ± 0.06 *	2.27 ± 0.01
Yield (Kg ha <sup>-1</sup> )	6,555.11 ± 301.82 *	4,138.34 ± 161.05

For each parameter, the mean values ± SE (n = 4) followed by \* indicates statistical differences between treatments at a 5% confidence level.

As regards the values observed by 66 DAS at leaf level, LT was similar between treatments, but  $I_G$  and SPAD values showed ca. 55% and 7% higher values, respectively, in D2 as compared with D7. In accordance with  $I_G$ , CWSI was higher (ca. 31%) for D7. Among the evaluations of light energy capture efficiency showed no significant differences between treatments for  $F_0$  and PI. However,  $F_0/F_m$  was higher in D2, whereas  $F_v/F_0$  and  $F_v/F_m$  were higher in D7 (Table 2).

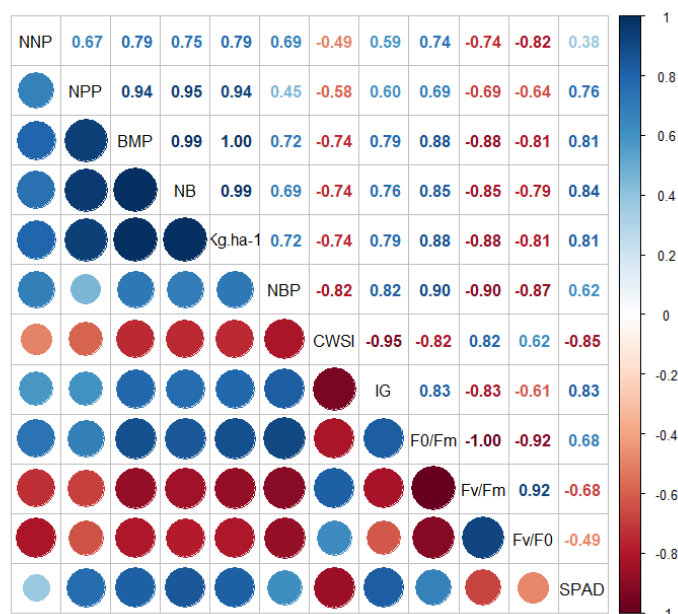
Table 2. Leaf temperature (LT), crop water stress index (CWSI), thermal relative stomatal conductance index ( $I_G$ ), initial fluorescence ( $F_0$ ), basal quantum yield of non-photochemical processes ( $F_0/F_m$ ), maximum quantum yield of photosystem II ( $F_v/F_m$ ), maximum efficiency of the photochemical process in photosystem II ( $F_0/F_v$ ), and Performance Index (PI), of *G. max* cv. Brasmax Olimpo IPRO sprayed with sugarcane molasses at 2 (D2) and 7 (D7) days after the onset of precipitation following a 28-day period without rain. Measurements were taken at 66 DAS.

Variables	D2	D7
LT	29.13 ± 0.13 <sup>ns</sup>	28.58 ± 0.18
CWSI	0.26 ± 0.007*	0.38 ± 0.02
$I_G$	3.97 ± 0.26*	1.77 ± 0.17
$F_0$	6926.48 ± 217.19 <sup>ns</sup>	6374.60 ± 103.13
$F_0/F_m$	0.21 ± 0.002*	0.19 ± 0.002
$F_v/F_m$	0.78 ± 0.002*	0.81 ± 0.002
$F_v/F_0$	3.79 ± 0.10*	4.21 ± 0.06
PI	3.42 ± 0.15 <sup>ns</sup>	4.26 ± 0.30
SPAD	44.98 ± 0.44*	42.15 ± 0.56

For each parameter, the mean values ± SE (n = 4) followed by either \* or ns indicates statistical differences and no statistical differences between treatments, respectively, at a 5% probability level.

To deeply explore our data, it was performed a phenotypic correlation among the variables, so that NNP exhibited positive correlation with others yield components, mainly with BMP and bean yield ( $r^2 = 0.79$ ). NPP demonstrated strong positive correlations with BMP, NB and bean yield (Figure 3). Conversely, CWSI,  $F_v/F_m$ , and  $F_v/F_0$  had negative correlations with yield components, mainly NBP ( $r^2 = -0.82$ ,  $-0.90$  and  $-0.87$ , respectively). In addition,  $I_G$ , SPAD reading and  $F_0/F_m$  demonstrated positive correlations with the variation of the yield components BMP, NB and bean yield (Figure 3).

Figure 3 - Estimates of phenotypic correlation among traits measured in *G. max* cv. Brasmax Olimpo IPRO plants sprayed with sugarcane molasses at 2 (D2) and 7 (D7) days after the onset of precipitation following a 28-day period without rain. The traits (only those that showed significant differences) assessed were number of nodes per plant (NNP), number of pods per plant (NPP), number of beans per plant (NB), number of beans per pod (NBP), bean mass per plant (BMP), bean yield (kg ha<sup>-1</sup>), crop water stress index (CWSI), thermal relative stomatal conductance index (I<sub>g</sub>), basal quantum yield of non-photochemical processes (F<sub>0</sub>/F<sub>m</sub>), maximum quantum yield of photosystem II (F<sub>v</sub>/F<sub>m</sub>), and maximum efficiency of the photochemical process in photosystem II (F<sub>v</sub>/F<sub>0</sub>). Areas of the circles show the value of corresponding phenotyping correlation coefficients. Correlation values are presented in the upper panel in squares; positive correlations are displayed in blue and negative correlations in red. Colour intensity (light to dark) and the size of the circle (small to big) are proportional to the correlation coefficients (0 to 1 for the positive coefficient and 0 to -1 for the negative coefficient).



## DISCUSSION

Our findings suggest management practices that may be suitable for post-stress recovery in soybean crops under field conditions. It is important to consider that, despite sporadic rainfall between December 2023 and early February 2024, the total rainfall since the beginning of the rainy season (October 2023) has significantly limited the amount of water stored in the soil compared to the 2022/2023 crop year (Figure 1). Therefore, these conditions exacerbated the stressful conditions during the experimental period. Interestingly, the results showed that sugarcane molasses application a shorter application interval (D2) significantly increased productivity components, *i.e.*, NNP, NPP, NB and NBP, which significantly contributed to the substantial increase in productivity (Table 1, Figure 3). It is worth noting that even the D7 treatment had higher productivity than the average observed across the state of Maranhão (3,312 kg ha<sup>-1</sup> in the 2023/2024, which could represent soybean plants that did not receive the sugarcane molasses application, as this is not yet

an established management practice). The question that arises is: what factors contributed to the higher productivity in D2?

Regarding the Chlorophyll *a* fluorescence, sugarcane molasses application a shorter application interval (D2) reduced  $F_v/F_0$  and  $F_v/F_m$ , while increased  $F_0/F_m$ , which could suggest some impact on the photochemical pathway (Table 2). However, the  $F_v/F_m$  values (indicating the maximum efficiency of quantum yield) fell within the range considered adequate for proper functioning of photosystem II, between 0.75 and 0.85 (Bolhàr-Nordenkampf *et al.* 1989). Although the  $F_v/F_0$  values (indicating maximum efficiency of the photochemical process in photosystem II and/or potential photosynthetic activity) were below 4, and  $F_0/F_m$  values were above 0.2, which may suggest a stress condition (Roháček, 2002; Zanandrea *et al.* 2006), PI values were similar between treatments, suggesting that the energy cascade processes, from initial absorption to plastoquinone reduction (Strasser *et al.* 2004), were comparable, indicating similar photochemical performance across treatments. Collectively, the fluorescence variable data also do not explain the observed productivity differences. It is worth noting that the negative correlations among yield components and  $F_v/F_m$  and  $F_v/F_0$  as well as positive correlations with  $F_0/F_m$  do not necessarily translate to a range of values beyond those observed in our study. For instance, under stress conditions  $F_v/F_m$  values below 0.75 are generally indicative of damage to the photosynthetic apparatus and reduced growth and productivity (Sommer *et al.* 2023). Therefore, caution should be exercised when interpreting these results.

A factor that may be associated with higher productivity in plants that received sugarcane molasses at a shorter interval after precipitation onset could be a faster recovery in the activity of enzymes related to nitrogen metabolism. Indeed, sugarcane molasses is rich in various micronutrients (Supplementary Table S1), such as iron, zinc, and manganese, which may enhance enzymatic activity (Ma *et al.* 2017; Kobayashi *et al.* 2019; Tavanti *et al.* 2021), thus supporting overall plant development. These micronutrients play crucial roles in enzymatic metabolism and chlorophyll formation, leading to higher levels of these pigments in plants treated with sugarcane molasses at a shorter interval (D2), as reflected by greater SPAD readings in this treatment (Table 2). In fact, there is a strong positive correlation between nitrogen and chlorophyll content with SPAD readings (Torres-Netto *et al.* 2005). Higher chlorophyll content increase the capacity for light absorption, which could potentially improve photochemical parameters (Abreu *et al.* 2022). However,

this was not observed in this case. Thus, we suggest that higher pigment content may have contributed to increased productivity at D2 in two ways: 1) by keeping leaves green for longer after the R5 stage, which could maintain photosynthetic capacity and supply photoassimilates for grain filling; and 2) by enhancing the ability to remobilize amino acids and nitrogen compounds, resulting in greater bean mass. In fact, higher green leaf area at R7 sustained a high rate of photoassimilate translocation to the reproductive parts in soybeans (Raza *et al.* 2021). This is further evidenced by a non-significant trend toward higher LAI in D2 treatment, as well as the strong correlation between SPAD values and yield and its components (Figure 1 and 3).

It was observed that the plot with sugarcane molasses applications at a longer interval exhibited a reduction in  $I_G$ , while had higher CWSI (Table 2), indicating more pronounced stomatal closure due to reduced water availability caused by water stress, resulting in a decrease in metabolic limitations (Silva *et al.* 2018). Thus, these responses are fundamental components of plant productivity, which explain the lower yield in the plot with sugarcane molasses application at a longer interval, considering the relative stomatal conductance.

The plot with sugarcane molasses applications at a shorter interval showed significant responses in terms of stomatal opening and closing, a process facilitated by K content in sugarcane molasses, which aids the stomatal complex and the functioning of the guard cell pair acting as a hydraulically operated valve (Sardans and Peñuela 2021). These responses were evidenced by the lower CWSI values and higher  $I_G$  values observed in the plot with sugarcane molasses application at a shorter interval (D2), as well as by phenotyping correlations (Figure 3).

In addition to enhancing stomatal opening, potassium plays a crucial role in improving reserve storage in beans by maintaining charge balance, which directly links ATP synthesis to potassium availability (Sardans and Peñuela, 2021). Therefore, the transport of energy from the source to the sink during grain filling is dependent on potassium, which impacted both the productivity and quality of the harvested beans.

In addition to potassium, the magnesium is essential for plants as it enhances the flow of sucrose from leaves to sink organs (Kleczkowski and Igamberdiev 2021; Ishfaq *et al.* 2022), well as it is a component of chlorophyll molecules, and plays roles in phosphorylation, photoassimilate translocation, and activation of multiple enzymes, such as glutathione synthetase and phosphoenolpyruvate carboxylase. Furthermore, magnesium

also helps regulate cell pH and charge balance, and is a constituent of ribosomes and chromosomes (Kleczkowski and Igamberdiev 2021). Therefore, higher productivity in molasses-treated plot at D2 can also be associated with improved photoassimilates translocation to the beans to some extent.

In summary, the results obtained in this study suggest that the use of sugarcane molasses as a means to remedy and improve plant conditions under water stress and high temperatures may be a viable strategy for producing soybeans in stressful environments where increased water-use efficiency may be required due to climate change. Furthermore, sugarcane molasses is a byproduct of sugar production in sugarcane mills, and thus, its use as a potential stress alleviator can contribute to environmental sustainability. Although our results indicate the benefits of using this product, further studies are needed to confirm the viability of this strategy, considering other stress conditions (intensity and duration) and phenological stages, as well as other cultivation conditions (environment and management).

## **CONCLUSIONS**

The molasses-treated plot at a shorter interval (D2) resulted in higher yield due to improved photoassimilate distribution and enhanced stomatal function, as reflected by the CWSI and  $I_G$  values. Together, these factors led to improved productivity components, particularly bean mass per plant. Overall, a phenotypic correlation was observed between yield components and  $I_G$  and SPAD, while a negative correlation was noted between yield components and CWSI. Finally, the application of sugarcane molasses at D2 likely reduced the duration in which the plant activated its response mechanisms for post-water stress recovery, allowing it to prioritize the reproductive process and thereby to reduce yield losses.

## **ACKNOWLEDGEMENTS**

The authors are grateful to Alto VR Agro Group for providing the space for the execution of the experiment.

## **FUNDING**

This study was funded by Universidade Estadual da Região Tocantina do Maranhão (UEMASUL) by fellowship awarded to WR (Call N° 14/2022 – CPG/PROPGI/UEMASUL),

and by Fundação de Amparo à Pesquisa e ao Desenvolvimento Científico e Tecnológico do Maranhão (FAPEMA) with fellowships granted to AS (BIC-02647/23) and MD (BIC-02549/23). Portuguese national funding support from Fundação para a Ciência e a Tecnologia, I.P. (FCT), through the projects CEF (UIDB/00239/2020, <https://doi.org/10.54499/UIDB/00239/2020>) and GeoBioTec (UIDP/04035/2020, <https://doi.org/10.54499/UIDB/04035/2020>), and Associate Laboratory TERRA (LA/P/0092/2020, <https://doi.org/10.54499/LA/P/0092/2020>) to J.C. Ramalho is also greatly acknowledged.

### **AUTHOR CONTRIBUTIONS**

Conceptualization, TCR, JCN, TMF, FOR, FAMAF, EC, JCR and WPR.; methodology, TCR, JCN, TMF, FOR, FAMAF, EC, and WPR; software, WPB, and WPR; validation, ASM, MDD, JSC, ALPS, NDRD, WPB, TCR, JCN, TMF, FOR, FAMAF, EC, and WPR; investigation, ASM, MDD, JSC, ALPS, NDRD, WPB, TCR, JCN, TMF, FOR, FAMAF, EC, JCR and WPR; writing—original draft, ASM, MDD, JSC, ALPS, NDRD, WPB, TCR, JCN, TMF, FOR, FAMAF, EC, JCR and WPR; writing—review and editing, TCR, JCN, TMF, FOR, FAMAF, EC, JCR and WPR; project administration, WPR. funding acquisition, WPR. All authors have read and agreed to the submitted version of the manuscript.

### **CONFLICT OF INTEREST**

All authors declare no conflict of interest.

### **DATA AVAILABILITY**

Data presented in this study will be available on a fair request to the corresponding author.

### **ETHICS APPROVAL**

Not applicable.

## REFERENCES

1. Arya, H., Singh, M. B., & Bhalla, P. L. (2021). Towards developing drought-smart soybeans. *\*Frontiers in Plant Science, 12\**, Article 750664. <https://doi.org/10.3389/fpls.2021.750664>
2. Abreu, D. P., Roda, N. M., De Abreu, G. P., Bernardo, W. P., Rodrigues, W. P., Campostrini, E., & Rakocevic, M. (2022). Kaolin film increases gas exchange parameters of coffee seedlings during transference from nursery to full sunlight. *\*Frontiers in Plant Science, 12\**, Article 784482. <https://doi.org/10.3389/fpls.2021.784482>
3. Alvares, C. A., Stape, J. L., Sentelhas, P. C., Moraes Gonçalves, J. L., & Sparovek, G. (2013). Koppen's climate classification map for Brazil. *\*Meteorologische Zeitschrift, 22\**(6), 711–728. <https://doi.org/10.1127/0941-2948/2013/0507>
4. Board, J. E., & Tan, Q. (1995). Assimilatory capacity effects on soybean yield components and pod number. *\*Crop Science, 35\**, 846–851. <https://doi.org/10.2135/cropsci1995.0011183X003500030034x>
5. Bolhár-Nordenkampf, H. R., Long, S. P., Baker, N. R., Öquist, G., Schreiber, U., & Lecher, E. G. (1989). Chlorophyll fluorescence as a probe of the photosynthetic competence of leaves in the field: A review of current instrumentation. *\*Functional Ecology, 3\**, 497–514. <https://doi.org/10.2307/2389624>
6. CONAB – Companhia Nacional do Abastecimento. (2024). *\*Boletim da Safra de Grãos\**. Available at: <https://www.conab.gov.br/info-agro/safras/graos/boletim-da-safra-de-graos> (Accessed 21 August 2024).
7. Diffenbaugh, N. S., & Burke, M. (2019). Global warming has increased global economic inequality. *\*Proceedings of the National Academy of Sciences, USA, 116\**, 9808–9813. <https://doi.org/10.1073/pnas.1816020116>
8. Egli, D. B. (2010). Soybean reproductive sink size and short-term reductions in photosynthesis during flowering and pod set. *\*Crop Science, 50\**, 1971–1977. <https://doi.org/10.2135/cropsci2009.12.0714>
9. FAO – Food and Agriculture Organization of the United Nations. (2016). *\*The State of Food and Agriculture Climate Change, Agriculture and Food Security\**. Food and Agriculture Organization, Rome, Italy.
10. Fischer, T., Byerlee, D., & Edmeades, G. (2014). *\*Crop Yields and Global Food Security: Will Yield Increase Continue to Feed the World?\** ACIAR, Grains Research and Development Corporation, Monograph, Canberra, Australia.
11. Fróna, D., Szenderák, J., & Harangi-Rákos, M. (2019). The challenge of feeding the world. *\*Sustainability, 11\**, Article 5816. <https://doi.org/10.3390/su11205816>
12. Galieni, A., D'Ascenzo, N., Stagnari, F., Pagnani, G., Xie, Q., & Pisante, M. (2021). Past and future of plant stress detection: An overview from remote sensing to positron

- emission tomography. \*Frontiers in Plant Science, 11\*, Article 609155. <https://doi.org/10.3389/fpls.2020.609155>
13. García-Tejero, I. F., Hernández-Cotán, A., Apolo, O. E., Durán-Zuazo, V. H., Portero, M. A., & Rubio-Casal, A. E. (2017). Infrared thermography to select commercial varieties of maize in relation to drought adaptation. \*Quantitative InfraRed Thermography Journal, 14\*, 54–67. <https://doi.org/10.1080/17686733.2017.1280338>
  14. Gilbert, M. E., Holbrook, N. M., Zwieniecki, M. A., Sadok, W., & Sinclair, T. R. (2011). Field confirmation of genetic variation in soybean transpiration response to vapor pressure deficit and photosynthetic compensation. \*Field Crops Research, 124\*, 85–92. <https://doi.org/10.1016/j.fcr.2011.06.014>
  15. Gupta, A., Rico-Medina, A., & Caño-Delgado, A. I. (2020). The physiology of plant responses to drought. \*Science, 368\*, 266–269. <https://doi.org/10.1126/science.aaz7614>
  16. Gutiérrez, S., Diago, M. P., Fernández-Novales, J., & Tardáguila, J. (2018). Vineyard water status assessment using on-the-go thermal imaging and machine learning. \*PLOS One, 13\*, Article e0192037. <https://doi.org/10.1371/journal.pone.0192037>
  17. IBGE – Instituto Brasileiro de Geografia e Estatística. (2024). \*Levantamento Sistemático da Produção Agrícola\*. Available at: <https://www.ibge.gov.br/estatisticas/economicas/agricultura-pecuaria> (Accessed 21 November 2024).
  18. IPCC. (2023). Sections. In \*Climate Change 2023: Synthesis Report\*. Contribution of Working Groups I, II and III to the Sixth Assessment Report of the Intergovernmental Panel on Climate Change [Core Writing Team, H. Lee, & J. Romero (eds.)]. IPCC, Geneva, Switzerland, 35–115. <https://doi.org/10.59327/IPCC/AR6-9789291691647>
  19. Ishfaq, M., Wang, Y., Yan, M., Wang, Z., Wu, L., Li, C., & Li, X. (2022). Physiological essence of magnesium in plants and its widespread deficiency in the farming system of China. \*Frontiers in Plant Science, 13\*, Article 802274. <https://doi.org/10.3389/fpls.2022.802274>
  20. Jones, H. G. (1992). \*Plants and Microclimate: A Quantitative Approach to Environmental Plant Physiology\* (2nd ed.). Cambridge University Press, Cambridge, United Kingdom.
  21. Kalaji, H. M., Jajoo, A., Oukarroum, A., Brestic, M., Zivcak, M., Samborska, I. A., Cetner, M. D., Łukasik, I., Goltsev, V., & Ladle, R. J. (2016). Chlorophyll a fluorescence as a tool to monitor physiological status of plants under abiotic stress conditions. \*Acta Physiologiae Plantarum, 38\*, Article 102. <https://doi.org/10.1007/s11738-016-2113-y>
  22. Kamphorst, S. H., Amaral Júnior, A. T., Lima, V. J., Santos, P. H. A. D., Rodrigues, W. P., Vivas, J. M. S., Gonçalves, G. M. B., Schmitt, K. F. M., Leite, J. T., Vivas, M., Mora-Poblete, F., Vergara-Díaz, O., Araus, O. J. L., Ramalho, J. C., & Campostrini, E. (2020). Comparison of selection traits for effective popcorn (*Zea mays* L. var. Everta) breeding



- under water-limiting conditions. \*Frontiers in Plant Science, 11\*, Article 1289. <https://doi.org/10.3389/fpls.2020.01289>
23. Kara, M., Seçgin, Z., Arslanoğlu, Ş. F., & Dinç, S. (2023). Endogenous food-borne sugar beet molasses carbon dots for alleviating the drought and salt stress in tobacco plant. \*Journal of Plant Growth Regulation, 42\*, 4541–4556. <https://doi.org/10.1007/s00344-023-10923-2>
24. Kleczkowski, L. A., & Igamberdiev, A. U. (2021). Magnesium signaling in plants. \*International Journal of Molecular Sciences, 22\*(3), Art. 1159. <https://doi.org/10.3390/ijms22031159>
25. Kobayashi, T., Nozoye, T., & Nishizawa, N. K. (2019). Iron transport and its regulation in plants. \*Free Radical Biology and Medicine, 133\*, 11–20. <https://doi.org/10.1016/j.freeradbiomed.2018.10.439>
26. Ma, D., Sun, D., Wang, C., Ding, H., Qin, H., Hou, J., Huang, X., Xie, Y., & Guo, T. (2017). Physiological responses and yield of wheat plants in zinc-mediated alleviation of drought stress. \*Frontiers in Plant Science, 8\*, Art. 860. <https://doi.org/10.3389/fpls.2017.00860>
27. NOAA – National Oceanic and Atmospheric Administration. (2024). Climate change: Atmospheric carbon dioxide. \*Climate.gov, USA.\* Available at: <https://www.climate.gov/news-features/understanding-climate/climate-change-atmospheric-carbon-dioxide> (Accessed November 2024).
28. Pais, I. P., Reboredo, F. H., Ramalho, J. C., Pessoa, M. F., & Lidon, F. C. (2020). Potential Impacts of Climate Change on Agriculture - A Review. \*Emirates Journal of Food and Agriculture, 32\*(6), 397–407. <https://doi.org/10.9755/ejfa.2020.v32.i6.2111>
29. Powell, N., Ji, X., Ravash, R., Edlington, J., & Dolferus, R. (2012). Yield stability for cereals in a changing climate. \*Functional Plant Biology, 39\*, 539–552. <https://doi.org/10.1071/FP12078>
30. R Core Team. (2021). R: A language and environment for statistical computing. \*R Foundation for Statistical Computing, Vienna, Austria.\* Available at: <https://www.R-project.org/>
31. Raza, M. A., Gul, H., Yang, F., Ahmed, M., & Yang, W. (2021). Growth rate, dry matter accumulation, and partitioning in soybean (*Glycine max L.*) in response to defoliation under high-rainfall conditions. \*Plants, 10\*, Art. 1497. <https://doi.org/10.3390/plants10081497>
32. Richter, G. L., Zanon, A. J., Streck, N. A., Guedes, J. V. C., Kräulich, B., da Rocha, T. S. M., Winck, J. E. M., & Cera, J. C. (2014). Estimativa da área de folhas de cultivares antigas e modernas de soja por método não destrutivo. \*Bragantia, 73\*, 416–425. <https://doi.org/10.1590/1678-4499.0179>

33. Rodrigues, A. P., Pais, I. P., Leitão, A. E., Dubberstein, D., Lidon, F. C., Marques, I., Semedo, J. N., Rakocevic, M., Scotti-Campos, P., Campostrini, E., Rodrigues, W. P., Simões-Costa, M. C., Reboredo, F. H., Partelli, F. L., DaMatta, F. M., Ribeiro-Barros, A. I., & Ramalho, J. C. (2024). Uncovering the wide protective responses in *Coffea* spp. leaves to single and superimposed exposure of warming and severe water deficit. *\*Frontiers in Plant Science, 14\**, 1320552. <https://doi.org/10.3389/fpls.2023.1320552>
34. Roháček, K. (2002). Chlorophyll fluorescence parameters: the definitions, photosynthetic meaning, and mutual relationships. *\*Photosynthetica, 40\**, 13–29. <https://doi.org/10.1023/A:1020125719386>
35. Sardans, J., & Peñuelas, J. (2021). Potassium control of plant functions: ecological and agricultural implications. *\*Plants, 10\**, Art. 419. <https://doi.org/10.3390/plants10020419>
36. Silva, J. R., Rodrigues, W. P., Ferreira, L. S., Bernado, W. P., Paixão, J. S., Patterson, A. E., Ruas, K. F., Viana, L. H., Sousa, E. F., Bressan-Smith, R. E., Ponie, S., Griffin, K. F., & Campostrini, E. (2018). Deficit irrigation and transparent plastic covers can save water and improve grapevine cultivation in the tropics. *\*Agricultural Water Management, 202\**, 66–80. <https://doi.org/10.1016/j.agwat.2018.01.002>
37. Sinclair, T. R. (2017). Soybean. In *\*Water-conservation traits to increase crop yields in water-deficit environments\** (pp. 17–26). Reino Unido: Springer.
38. Sirault, X. R. R., James, R. A., & Furbank, R. T. (2009). A new screening method for osmotic component of salinity tolerance in cereals using infrared thermography. *\*Functional Plant Biology, 36\**, 970–977. <https://doi.org/10.1071/FP09145>
39. Sommer, S. G., Han, E., Li, X., Rosenqvist, E., & Liu, F. (2023). The chlorophyll fluorescence parameter Fv/Fm correlates with loss of grain yield after severe drought in three wheat genotypes grown at two CO<sub>2</sub> concentrations. *\*Plants, 12\**, Art. 436. <https://doi.org/10.3390/plants12030436>
40. Strasser, R. J., Srivastava, A., & Tsimilli-Michael, M. (2004). Analysis of the chlorophyll a fluorescence transient. In *\*Chlorophyll fluorescence: A signature of photosynthesis. Advances in photosynthesis and respiration\** (pp. 321–362). Dordrecht, The Netherlands: Kluwer Academic Publishers.
41. Tavanti, T. R., Melo, A. A. R., De Moreira, L. D. K., Sanchez, D. E. J., Silva, R. S., Silva, R. M., & Reis, A. R. (2021). Micronutrient fertilization enhances ROS scavenging system for alleviation of abiotic stresses in plants. *\*Plant Physiology and Biochemistry, 160\**, 386–396. <https://doi.org/10.1016/j.plaphy.2021.01.040>
42. Torres Netto, A., Campostrini, E., Oliveira, J. G., & Bressan-Smith, R. E. (2005). Photosynthetic pigments, nitrogen, chlorophyll a fluorescence and SPAD-502 readings in coffee leaves. *\*Scientia Horticulturae, 104\**, 199–209. <https://doi.org/10.1016/j.scienta.2004.08.013>

43. USDA – United States Department of Agriculture. (2024). Production Data – Commodity Report. Available at: <https://fas.usda.gov/data/production/commodity/2222000> (Accessed 19 November 2024).
44. Wind, J., Smeekens, S., & Hanson, J. (2010). Sucrose: metabolite and signaling molecule. \*Phytochemistry, 71\*, 1610–1614. <https://doi.org/10.1016/j.phytochem.2010.07.026>
45. Zanandrea, I., Nassi, F. L., Turchetto, A. C., Braga, E. J. B., Peters, J. A., & Bacari, M. A. (2006). Efeito da salinidade sob parâmetros de fluorescência em *Phaseolus vulgaris*. \*Revista Brasileira de Agrociência, 12\*, 157–161.
46. Zhao, C., Liu, B., Piao, S., Wang, X., Lobell, D. B., Huang, Y., Huang, M., Yao, Y., Bassu, S., Ciais, P., Durand, J. L., Elliott, J., Ewert, F., Janssens, I. A., Li, T., Lin, E., Liu, Q., Martre, P., Müller, C., Peng, S., Peñuelas, J., Ruane, A. C., Wallach, D., Wang, T., Wu, D., Liu, Z., Zhu, Y., Zhu, Z., & Asseng, S. (2017). Temperature increase reduces global yields of major crops in four independent estimates. \*Proceedings of the National Academy of Sciences, 114\*(35), 9326–9331. <https://doi.org/10.1073/pnas.1701762114>
47. Zia, S., Romano, G., Spreer, W., Sanchez, C., Cairns, J., Araus, J. L., & Müller, J. (2013). Infrared thermal imaging as a rapid tool for identifying water-stress tolerant maize genotypes of different phenology. \*Journal of Agronomy and Crop Science, 199\*, 75–84. <https://doi.org/10.1111/j.1439-037X.2012.00537.x>

## SUPPLEMENTARY MATERIAL

Table S1 - Composition of sugarcane molasses used in the experiment. Source: Comércio de Melaço de cana ECL LTDA.

Variable	Value
Brix (°)	81.0
Total Reducing Sugars (g/100 mL)	59.7
Water – Karl Fischer	19.34% (w/w)
Purity	43.4%
Starch	1709 (µg/g)
Fructose	7.5% (w/w)
Glucose	5.5% (w/w)
Dextrin	< 10 (µg/g)
Sucrose	39.9% (w/w)
Total Carbon	30%
Dry Matter	73.2%
Calcium	11455 (µg/g)
Crude Protein	4.3%
Crude Fiber	0.05%
Mineral Matter	8.5%
Copper	3.60 (µg/g)
Density	1.40 Kg/L
Iron	62.0 (µg/g)
Magnesium	4150 (µg/g)
Manganese	28.0 (µg/g)
Potassium	25570 (µg/g)
Sodium	119 (µg/g)
Zinc	6.2 (µg/g)
Cobalt	1.50 (µg/g)
Total Phosphorus	1.26 (mg/L)
Non-nitrogenous Extract	87.2%
Ash	9.0% (w/v)
Total Acidity – (acetic acid)	1.2 (mg/g)
pH	5.7